THE JOURNAL OF BIOLOGICAL CHEMISTRY VOL. 281, NO. 45, pp. 33959–33970, November 10, 2006

Glucocorticoids Repress *bcl-X* Expression in Lymphoid Cells by Recruiting STAT5B to the P4 Promoter*

Received for publication, March 14, 2006, and in revised form, September 7, 2006 Published, JBC Papers in Press, September 7, 2006, DOI 10.1074/jbc.M602408200

Luciana Rocha-Viegas[‡§1], **Guillermo P. Vicent**[§], **José L. Barañao**[¶1], **Miguel Beato**[§], **and Adali Pecci**[‡¶1,2]

From the Departamentos de [¶]*Química Biológica y* [‡]*Fisiología, Biología Molecular y Celular, Instituto de Fisiología, Biología Molecular y Neurociencias (IFIBYNE)-Consejo Nacional de Investigaciones Científicas y Técnicas, Facultad de Ciencias Exactas y Naturales, Universidad de Buenos Aires, Ciudad Universitaria, Intendente Güiraldes 2160, Pab. II, 2do piso, C1428EGA Buenos Aires, Argentina and the* [§]*Centre de Regulació Genòmica, Universitat Pompeu Fabra, Passeig Marítim, 37-49, 08003 Barcelona, Spain*

The *bcl-X* gene plays a critical role in apoptosis. Six different isoforms generated by tissue-specific promoter usage and alternative splicing were described. Some of them exert opposite effects on cell death. In mammary epithelial cells glucocorticoids induce *bcl-X* expression and increase the ratio *bcl-X_L* (antiapoptotic)/*bcl-X_S* (apoptotic) by activating P4 promoter, which contains two hormone response elements. Here we show that, on mouse thymocytes and T lymphocyte derivative S49 cells, glucocorticoids inhibited transcription from P4 and decreased the ratio *bcl-X_L*/*bcl-X_S* favoring apoptosis. Upon hormonal treatment, glucocorticoid receptor (GR), steroid receptor coactivator-1, and RNA polymerase II were transiently recruited to P4 promoter, whereas STAT5B was also recruited but remained bound. Concomitant with the release of GR, silencing mediator for retinoic acid receptor and thyroid hormone receptor and histone deacetylase 3 were recruited, histone H3 was deacetylated, and RNA polymerase II left the promoter. Inhibition of STAT5 activity reverted glucocorticoid repression to activation of transcription and was accompanied by stable recruitment of GR and RNA polymerase II to P4.

Glucocorticoids have tissue-specific effects on apoptosis and cell survival. In monocytes, macrophages, and T lymphocytes they induce apoptosis (1), whereas they protect against apoptotic signals evoked by different stimuli in mammary epithelial cells (2, 3), endometrium (4), ovarian follicle (5), hepatocytes (6), and fibroblasts (7). Several reports suggested that the opposite control of apoptosis by glucocorticoids is exerted by modulation of a few genes, such as *bcl-2*, *bcl-X*, *bax*, and *NFκB*, in a cell type-specific manner (1, 4, 8, 9). These multiple effects could be achieved by composite regulatory cross-talk between GR[3] and a variety of nuclear modulators, which are selectively involved in the hormone-dependent expression of specific genes.

One of the key genes mediating steroid hormone effects is *bcl-X*, a member of the Bcl-2 family, which plays a critical role in the control of programmed cell death. Six different Bcl-X isoforms can be generated by alternative splicing. Some of them exert opposite effects on apoptosis (10–14); *i.e.* the large isoform Bcl-X_L protects cells against death (10), whereas the short isoform Bcl-X_S antagonizes cell death inhibition by interacting with Bcl-X_L and Bcl-2 (10).

In previous works with mammary and endometrial epithelial cells, we have shown that glucocorticoids exert an antiapoptotic effect mediated by the induction of *bcl-X* expression and an increase in the ratio *bcl-X_L*/*bcl-X_S* (4, 15). However, in thymocytes, glucocorticoids increase apoptosis by inhibiting *bcl-X* expression and decreasing the ratio *bcl-X_L*/*bcl-X_S* (16, 17). The 5′ upstream region of the mouse *bcl-X* gene contains five different promoters, which exhibit a tissue-specific pattern of promoter usage (18). Recently, we described two HREs located immediately upstream of P4, which bind GR and confer hormone responsiveness to the core promoter (15). Only P4 is activated upon hormone treatment of the mammary epithelial HC11 cell line, and this effect correlates with an increased *bcl-X_L* mRNA, suggesting that the antiapoptotic effect of glucocorticoids in this cellular context involves a direct induction of *bcl-X_L* through the activation of P4 (15).

To test whether a similar mechanism is involved in the hormonal regulation of cell types where glucocorticoids induce apoptosis, we performed *in vivo* analysis of *bcl-X* expression on thymocytes of mice treated with Dex for its physiological relevance, and on the T lymphocyte derivative S49 cell line, which is known to respond to glucocorticoids with programmed cell death (19, 20). It was previously shown that *bcl-X* expression decreases during the apoptotic process in thymocytes (8, 16, 17, 21). Only the levels of transcripts generated from P4, but not those derived from the other four promoters, were decreased in response to hormone in both the thymus and murine T lymphocyte S49 cell line. ChIP assays showed a transient loading of

* This work was supported in part by the Ministry of Education and Science (Grant SAF2001-0463 to M. B.) and grants from Consejo Nacional de Investigaciones Científicas y Técnicas (CONICET), University of Buenos Aires, and the National Agency of Scientific Promotion (Grant BID-1201 PICT 05-09044 to A. P.). The costs of publication of this article were defrayed in part by the payment of page charges. This article must therefore be hereby marked "*advertisement*" in accordance with 18 U.S.C. Section 1734 solely to indicate this fact.

[1] Members of CONICET.

[2] To whom correspondence should be addressed. Tel.: 54-11-4576-3300 (ext. 483); Fax: 54-11-4576-3342; E-mail: apecci@qb.fcen.uba.ar.

[3] The abbreviations used are: GR, glucocorticoid receptor; STAT5A, -B, signal transducer and activator of transcription 5 a/b; SRC-1, steroid receptor coactivator-1; SMRT, silencing mediator for retinoic acid receptor and thyroid hormone receptor; HDAC-3, histone deacetylase 3; NF-κB, nuclear factor kappa B; HRE, hormone response element; ChIP, chromatin immunoprecipitation; pol II, RNA polymerase II; Dex, dexamethasone; RU486, RU-38486; TSA, Tricostatin A; GAPDH, glyceraldehyde-3-phosphate dehydrogenase; BRG-1, brahma-related gene 1; EMSA, electrophoretic mobility shift assay; JAK, Janus-associated kinase; NF1, nuclear factor 1; GILZ, glucocorticoid-induced leucine zipper; nt, nucleotide(s); wt, wild type.

GR to the HREs accompanied by a stable recruitment of STAT5B at a potential binding site located between the HREs and the P4 TATA box. Concomitant with the release of GR, SMRT and HDAC3 were recruited, histone H3 was deacetylated, and pol II left the P4 region. Inhibition of STAT5 activity restored not only the increased occupancy by pol II, but also the stable binding of GR at the P4 region and the consequent induction of transcription. These results suggest that glucocorticoids repress *bcl-X* expression in thymocytes via cross-talk with STAT5B and contribute to the understanding of the molecular basis for tissue-specific hormonal effects on apoptosis.

EXPERIMENTAL PROCEDURES

Steroids and Reagents—Dex (10 nM), RU486 (1 μM), and RPMI 1640 medium were purchased from Sigma. Dulbecco's modified Eagle's medium, horse serum, and fetal calf serum were purchased from Invitrogen. Fetal calf serum was previously charcoal-stripped to deplete it of steroid hormones (22). The inhibitor AG490 (100 μM) was purchased from Calbiochem.

Plasmid Constructions—The vector pP4-extended (expressing luciferase under the control of *bcl-X* P4 promoter), pNM1–9SalI, pNM1–9SacI-EcoRI and pNM1–9EagI were described before (15). pP4ΔSTAT5 was generated by mutating (by PCR) the nucleotides located at −240, −239, −238, and −234 to adenines relative to the P4 transcription start site. The plasmid pBKSP4 was generated by amplifying from pNM1–9SalI plasmid, a fragment of 143 bp with the oligonucleotide 5′-*exonD*: 5′-CCAGGATCTGAGTTCCACTCTTGAACAGAATAA-CGC-3′ corresponding to the nucleotides −2694 to −2658 and the oligonucleotide 3′-*exonD*: 5′-AAATGAGCTATAA-CTCAGTTTTTCAA-3′ corresponding to the nucleotides −2551 to −2577 as forward and reverse primers, respectively. The PCR product was blunted, cut with SpeI, and then cloned into SpeI and EcoRV sites of pBluescript KS$^-$.

Animal Treatment—Male CF-1 mice of 20-g body weight were injected with Dex (0.5 mg/100 g body weight in 0.2 ml of vehicle: ethanol:propyleneglycol:NaCl (0.9%), 3:3:34) intraperitoneally. This dose is able to induce internucleosomal DNA fragmentation (16). RU486 (0.5 mg/100 g body weight in 0.2 ml of corn oil) was injected subcutaneously 45 min before Dex. Mice injected with vehicle alone were used as control. All animals were treated and cared for in accordance with standard international animal care protocols (23). Animals were sacrificed by cervical dislocation at different times, according to the subsequent analysis, and thymuses were excised. The thymocyte isolation was performed according to Hoijman *et al.* (9) and Vicent *et al.* (16).

Cell Cultures and Transfection Assays—Cells were cultured at 37 °C under humidified atmosphere with 5% CO_2 in p100 plates. COS-1 cells were grown in Dulbecco's modified Eagle's medium supplemented with 10% fetal calf serum containing penicillin (100 IU/ml), streptomycin (100 μg/ml), and glutamine (2 mM). S49 cells from mouse T lymphoma were grown in Dulbecco's modified Eagle's medium supplemented with 10% horse serum and 1% penicillin/streptomycin. For transient transfections 5×10^5 cells plated in 60-mm plates were transfected with Lipofectin 2000 (Invitrogen) following the instructions of the manufacturer. 3 μg of pP4-extended reporter vector (15) or pP4ΔSTAT5 (P4 reporter vector with four point mutations on the STAT5 site) and 1 μg of pGR (24) were co-transfected into COS-1 cells with increasing amounts of constitutively active mutants of STAT5B (pSTAT5B-N642H) and STAT5A (pSTAT5A-N642H) vectors (kindly provided by T. Kitamura (25)). 3 μg of pCMV-LacZ were also used as control of transfection. The plasmids were diluted in 100 μl of medium and added dropwise to an equal volume of medium containing 4 μl of Lipofectin 2000 (Invitrogen). After 20 min, the transfection mixture was added dropwise to the cells. 6 h later, the medium was replaced by medium containing 10% charcoal-stripped FCS and the antibiotics described above, and the mixture was incubated overnight at 37 °C in a 5% CO_2 atmosphere. The cells were then incubated with Dex for 36 h. After incubations, cells were harvested in lysis buffer (Promega, Madison, WI, cat. no. E3971), and luciferase activity was measured with a luciferase kit according to the manufacturer protocol (Promega, cat. no. E1501). β-Galactosidase activity was measured as described before (26). The JAK inhibitor AG490 (100 μM) was added 2 h before Dex, and the HDAC inhibitor TSA (16 μM) was added 30 min before Dex.

RNA Analysis—Animals were injected with vehicle or Dex for 2 h, sacrificed, and thymuses were excised. In addition, S49 cells were treated with or without Dex during 5 h. RNA was extracted by the single step method (27). RNase protection analysis was performed as described before (28). The *bcl-X* coding region probe was prepared from plasmid pGLD3 (kindly provided by J. M. Hardwick, The Johns Hopkins Hospital, Baltimore, MD), which was digested with HinfI and transcribed by T3 RNA polymerase. The full-length transcript size of the *bcl-X* Riboprobe was 294 nt, and the protected fragments for *bcl-*X_L and *bcl-*X_S were 237 and 155 nt long, respectively. For preparing the P1 Riboprobe, plasmid pNM1–9SalI (15) was digested with MaeIII and transcribed by T3 RNA polymerase. The full-length transcribed Riboprobe was 558 nt, and the protected fragment was 176 nt. For preparing the P2 Riboprobe, plasmid pNM1–9EagI (15) was digested with EcoRI and transcribed by T7 RNA polymerase; the full-length transcribed Riboprobe was 495 nt, and the protected fragment was 124 nt long. P4 Riboprobe was prepared by cutting the plasmid pBKSP4 with SpeI and transcribed with T3 RNA polymerase. The full-length transcribed Riboprobe was 207 nt, and the protected fragment was 147 nt long. For preparing the P5 Riboprobe plasmid, pNM1–9SacI-EcoRI was digested with SacI and transcribed with T3 RNA polymerase; the full-length Riboprobe was 670 nt long, and the protected fragment was 248 nt long. The *GAPDH* template pTRIGAPDH (Ambion, Austin, TX) was digested with BglII and transcribed with T3 RNA polymerase as described previously (4). The probe length was 359 nt, and the size of the protected fragment was 316 nt. [α-^{32}P]CTP (Amersham Biosciences) radiolabeled RNA probes were prepared using a kit according to the instructions of the manufacturer (Promega). The probes were co-precipitated with RNA samples and dissolved in hybridization buffer, denatured at 95 °C for 10 min, and hybridized at 52 °C for 18 h. After digestion with RNases A and T1, followed by digestion with proteinase K, the samples

were precipitated, denatured, and subjected to electrophoresis on a 5% denaturing acrylamide gel.

For reverse transcription, 4 μg of total RNA were used. The first cDNA strand was synthesized with Superscript reverse transcriptase and 25 ng/μl oligo(dT) (Invitrogen) as reverse complementary primer. For PCR amplification of the P4 5′-leading exon, the oligonucleotide 5′-*exonD*: (5′-CCAGGATCTGAGTTCCACTCTTGAACAGAATTAACGC-3′) corresponding to the nucleotides −2694 to −2658 from ATG and the oligonucleotide 3′-*exonD*: (5′-AAATGAGCTATAACTCAGTTTTTCAA-3′) corresponding to the nucleotides −2551 to −2577 from ATG were used as forward and reverse primers, respectively. The reaction yielded a 143-bp length cDNA fragment. PCRs were normalized against *GAPDH* expression. Primers *GAPDH-for* (5′-TCATCAACGGGAAGCCCATCACCATCTTC-3′) and *GAPDH-rev* (5′-GTCTTCTGGTTGGCAGTAATGGCATGGACT-3′), which specifically hybridize with *GAPDH* mRNA, were used. The reaction yielded a 357-bp length cDNA fragment. PCRs were normalized against *GAPDH* expression. Primers *GAPDH-for* (5′-TCATCAACGGGAAGCCCATCACCATCTTC-3′) and *GAPDH-rev* (5′-GTCTTCTGGTTGGCAGTAATGGCATGGACT-3′), which specifically hybridize with *GAPDH* mRNA, were used. To achieve semiquantitative conditions, reverse transcriptase-PCRs were terminated and the products were quantified when all of the samples were in the linear range of amplification. The cDNA pool (2 μl), 1.25 units of *Thermus aquaticus Taq* polymerase (Invitrogen), and amplification primers (20 pmol of each) in 50 μl of PCR mixture (1 μl of polymerase buffer, 2 mM $MgCl_2$, 200 μM each dNTP) denatured 3 min at 96 °C followed by 8, 15, 25, and 30 cycles of amplification by using a step program (96 °C for 40 s; 65 °C (for *GAPDH*) and 60 °C (for *exonD*) for 30 s; and 72 °C for 1 min) and a final extension at 72 °C for 10 min. PCR products were analyzed by electrophoresis in 1.6% agarose gels and visualized under UV light. Quantification was performed with a phosphorimaging device (Fuji FLA 3000G) using ImageGauge software. In all cases the quantification was normalized against the *GAPDH* signal.

ChIP Assays—S49 cells were untreated or incubated for different times (from 0 to 30 min) with 10 nM Dex, and ChIP assays were performed as described previously (29, 30). In addition, animals were injected with vehicle or Dex for 30 min, sacrificed, and thymuses were excised. Thymocytes were dispersed in 2 ml of phosphate saline buffer; then 220 μl of cross-linking solution (50 mM HEPES, pH 8; 0.1 M NaCl; 1 mM EDTA; 0.5 mM EGTA; 11% formaldehyde) was added to the samples, and they were incubated for 10 min at 37 °C. ChIP assays were then performed as above. The following antibodies were used: mouse monoclonal α-GR (BuGR, Affinity Bioreagents, Golden, CO), mouse monoclonal α-pol II (8WG16, Berkeley Antibody Co.), mouse monoclonal α-STAT5B (G-2, Santa Cruz Biotechnology, Santa Cruz, CA), rabbit polyclonal α-STAT5A (L-20, Santa Cruz Biotechnology), mouse monoclonal α-SRC1 (Upstate Biotechnologies), rabbit polyclonal α-SMRT (Santa Cruz Biotechnology), rabbit polyclonal α-BRG-1 (Santa Cruz Biotechnology), rabbit polyclonal α-HDAC3 (Abcam), and rabbit polyclonal α-acetylhistone H3 (Upstate Biotechnologies). Control for nonspecific interaction of DNA was performed by using as nonspecific antibody normal rabbit and mouse IgG (data not shown). For each experiment, PCRs were performed with different numbers of cycles or with dilution series of input DNA to determine the linear range of amplification; all results shown fall within this range. Primer sequences are available on request. The density of bands was quantified with Image J software (version 1.35s, 2005).

In Silico Analysis—Screening for potential transcription factor binding sites was performed using MatInspector software (31).

Protein Analysis—Protein extracts were prepared by lysing cells as described before (9). Protein concentration was measured by Bradford assay (Bio-Rad). For co-immunoprecipitation assays mouse polyclonal α-STAT5B (Santa Cruz Biotechnology) was used. Protein extract (0.6 mg) was incubated overnight with 2 μg of antibody at 4 °C on a vertical rotator. Protein A/G-Sepharose beads (Santa Cruz Biotechnology) were added, and the mixture was incubation continued for 1 h. Samples were washed three times with lysis buffer and resuspended in 2× sample buffer (250 mM Tris-HCl, pH 6.8, 4% SDS, 10% glycerol, 2% β-mercaptoethanol, 0.006% bromphenol blue). For Western blots, samples were boiled for 5 min and applied on a 15% SDS-polyacrylamide gel, and electrophoresis was performed at 25 mA for 2 h. The resolved proteins were transferred to a Hybond ECL membrane (Amersham Biosciences) by electroblotting. Antibody incubation was performed in blocking buffer (1% skim milk, 0.5% Tween) in Tris-buffered saline at 4 °C. As primary antibodies, the rabbit polyclonal α-STAT5A, the mouse monoclonal α-STAT5B described before, the rabbit polyclonal α-Bcl-$X_{L/S}$, and the mouse monoclonal α-phosphorylated tyrosine were applied (Santa Cruz Biotechnology). For tubulin expression the rabbit polyclonal γ-tubulin antibody (Santa Cruz Biotechnology) was used. As secondary antibody, a peroxidase-labeled α-rabbit or α-mouse antibody, was used (Amersham Biosciences). Proteins bands were detected using the ECL kit (Amersham Biosciences).

Electrophoretic Mobility Shift Assay—EMSAs were performed with the 303-bp oligonucleotide *bclX*-P4 wild type or mutated, generated by digesting pP4-extended or pP4ΔSTAT5 vector, between the nucleotides −3133 and −2829, with AseI and BglII enzymes. Nuclear extracts from S49 cells treated for 30 min with Dex (10 nM) were prepared as previously described (32). Binding reactions were carried out according to our previous description (15). Results were visualized by autoradiography of the dried gel and analyzed using a phosphorimaging device (Fuji FLA 3000G) and quantification software (ImageGauge version 3.1). The monoclonal α-GR antibody (BuGR, Affinity Bioreagents) and the polyclonal α-STAT5A and monoclonal α-STAT5B antibodies (Santa Cruz Biotechnology) were included in the incubation mixture for supershift assays.

Statistical Analysis—Statistical analysis was performed by using the two-way analysis of variance followed by Turkey's test using GraphPad Instat software (version 3.01, 1998).

RESULTS

Dex Decreases the Levels of bcl-X Transcripts in Thymocytes through the Inhibition of P4 Activity—Lymphoid cells, especially thymocytes, undergo apoptosis in response to glucocor-

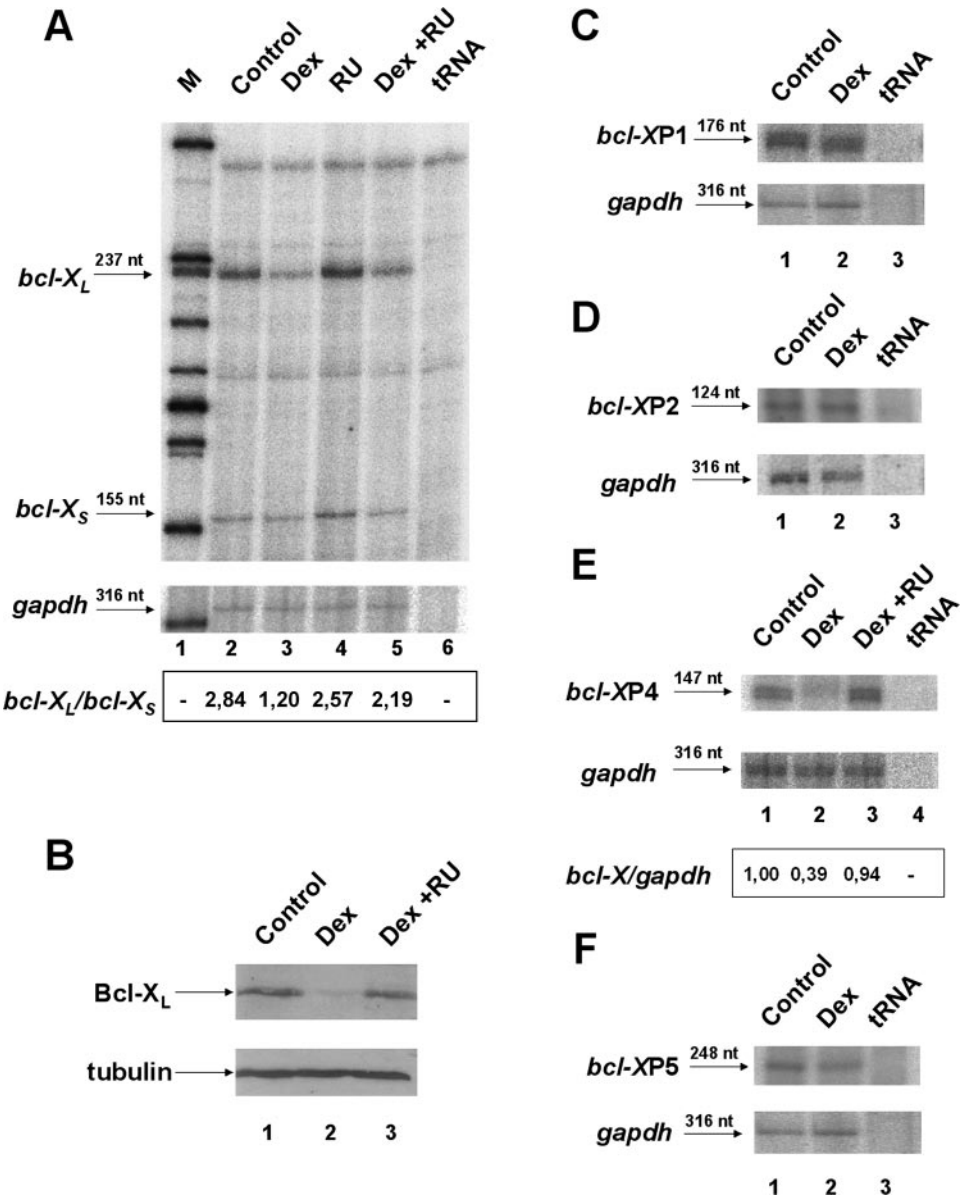

FIGURE 1. *A*, RNase protection assay of total RNA harvested from thymocytes of control animals (*lane 2*), treated with Dex (*lane 3*), with RU486 (*lane 4*), or with RU486 plus Dex (*lane 5*). The protected bands of long and short isoforms are indicated by *arrows*. *Lane 6*, tRNA as negative control; *lane 1*, molecular weight marker. The ratio *bcl-X*$_L$/*bcl-X*$_S$ is indicated at the *bottom* of the figure. *B*, Western blot of Bcl-X$_L$. Protein extract from thymocytes of control animals (*lane 1*), treated with Dex (*lane 2*), or with RU486 plus Dex (*lane 3*). Tubulin expression was used as control. *C–F*, RNA transcripts from P1 (*C*), P2 (*D*), P4 (*E*), and P5 (*F*) from control animals (*lane 1*) or treated with Dex (*lane 2*). tRNA as negative control (*lane 3* in *B*, *C*, and *E* and *lane 4* in *D*). *E*, *lane 3*, RU486 plus Dex treatment. *GAPDH* expression was used as control. The values are expressed as -fold induction relative to the controls at the bottom of *panel E*. The results correspond to representative gels from three independent experiments. *nt*, nucleotides.

ticoids. It was previously shown that the relative abundance of *bcl-X* isoforms changes during the apoptotic process (8, 16, 17, 21). We first examined by RNase protection assays the expression levels of the *bcl-X*$_L$ and *bcl-X*$_S$ isoforms in thymocytes of animals treated for 2 h with Dex. In thymus from untreated mice both isoforms are expressed at the ratio *bcl-X*$_L$/*bcl-X*$_S$ = 2.8 ± 0.1 (Fig. 1*A*, *lane 2*). The level of *bcl-X*$_L$ was drastically decreased upon hormonal treatment, which had little effect on the levels of *bcl-X*$_S$ transcripts being the ratio *bcl-X*$_L$/*bcl-X*$_S$ = 1.2 ± 0.1 (Fig. 1*A*, *lane 3*). This effect was likely mediated by GR, because it was inhibited in the presence of the GR antagonist, RU486, which restored the *bcl-X*$_L$/*bcl-X*$_S$ ratio to 2.3 ± 0.2 (Fig. 1*A*, *lane 5*). Treatment with RU486 had neither significant effect on transcript levels nor on the ratio of both isoforms (Fig. 1*A*, *lane 4*). Similar results were previously observed in rat thymocyte primary cultures treated with glucocorticoids (16). The levels of Bcl-X$_L$ protein also decreased after 8 h of Dex injection (Fig. 1*B*, *lane 2*). The co-injection of the antagonist RU486 abolished this effect (Fig. 1*B*, *lane 3*). We conclude that glucocorticoids affect *bcl-X*$_L$ transcript and Bcl-X$_L$ protein levels in thymocytes in a way compatible with their proapoptotic effect in these cells.

To determine which of the various *bcl-X* promoters was responsible for the hormonal decrease in *bcl-X* transcripts, we performed RNase protection assays using specific Riboprobes for the different 5′-leading exons. Hormone treatment had no effect on transcripts generated from promoters P1, P2, or P5 (Fig. 1, *C*, *D*, and *F*, respectively). In contrast, the level of transcripts containing the 5′-leading exon of P4 decreased 2.6 ± 0.2-fold *versus* control (ratio *bcl-X P4*/*GAPDH* = 1.0 ± 0.1), in thymus samples obtained from animals treated with Dex (ratio *bcl-X P4*/*GAPDH* = 0.4 ± 0.1) (Fig. 1*E*, *upper panel*, *lanes 1* and *2*, respectively). The hormone effect was abolished by the co-injection of RU486 (ratio *bcl-X P4*/*GAPDH* = 0.9 ± 0.1) (Fig. 1*E*, *upper panel*, *lane 3*). As control, no change was detected in *GAPDH* RNA levels after hormone treatment (Fig. 1*E*, *lower panel*). Transcripts generated from P3 were not analyzed, because this promoter is completely inactive in thymocytes (18). We conclude that the changes in *bcl-X* expression reflect an effect of the hormone on the accumulation of transcripts derived from P4.

These changes in *bcl-X* transcript levels could result from a decrease in the transcription rate or in the stability of the transcripts. We therefore tested whether the *bcl-X* P4 region was occupied by the transcriptional machinery after hormone treatment. ChIP assays using a monoclonal pol II antibody demonstrated the presence of the enzyme bound to the P4 region in thymocytes obtained from untreated mice (2.1%

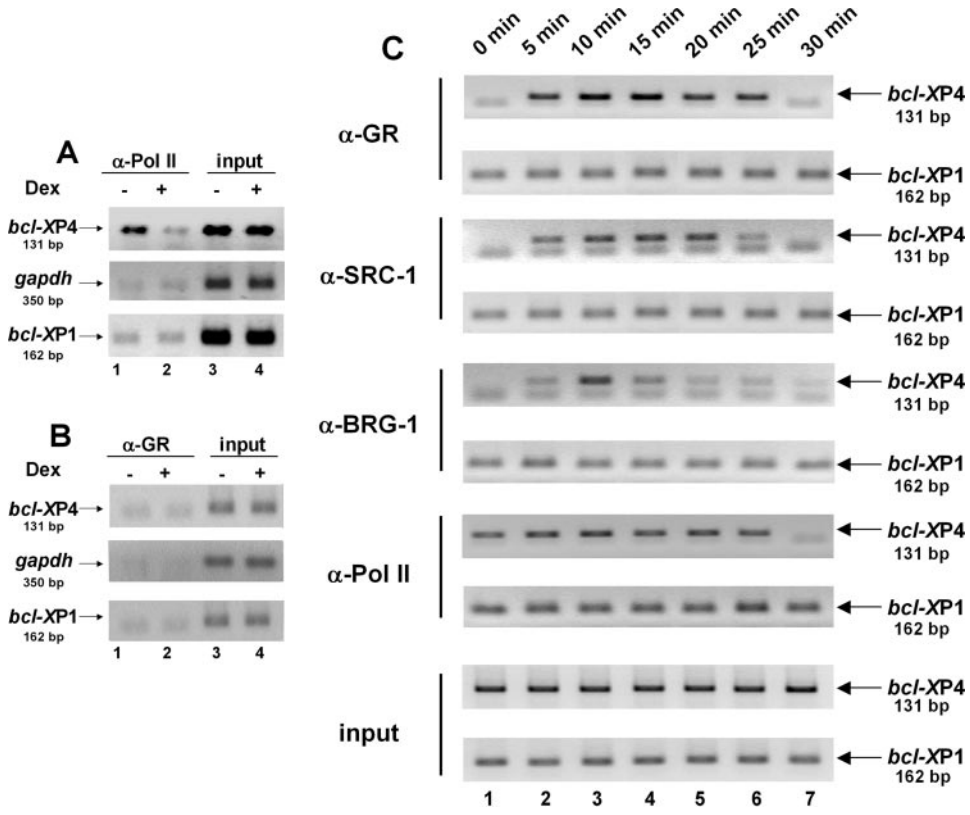

FIGURE 2. **Binding of pol II and GR to P4 region.** Thymocytes belonging to animals treated for 30 min with Dex (*lane 2*) or control (*lane 1*) were analyzed for binding of pol II (*A*) and GR (*B*) to *bcl-X* P4 (*upper panels*) and to the *bcl-X* P1 region (*lower panels*) by ChIP assays. *Lanes 3* and *4*, input chromatin. *GAPDH* gene amplification was used as control (*middle panels*). The results correspond to representative gels from three independent experiments. *C*, kinetics of transcription factors and co-regulators binding to P4. S49 cells incubated from 5 to 30 min with Dex (*lanes 2–7*). Binding of GR, SRC-1, BRG-1, and pol II to *bcl-X* P4 (*odd panels*) and P1 regions (*even panels*) determined by ChIP assays. Input chromatin is shown in the *last panels*. The results correspond to representative gels from three independent experiments. *bp*, base pairs.

DNA bound) (Fig. 2*A*, *upper panel*, *lane 1*), as expected given the basal activity of the promoter. After 30 min, the hormonal treatment reduced the levels of pol II bound to P4 region (0.84% DNA bound) (Fig. 2*A*, *upper panel*, *lane 2*). These findings suggest that the glucocorticoid-induced changes in transcript levels are mediated by P4 repression. Treatment with Dex did not influence the binding of pol II to the *bcl-X* proximal promoter region, whose basal recruitment was lower than that observed in P4 (0.51% DNA bound) (Fig. 2*A*, *lower panel*). The *GAPDH* gene was used as control (Fig. 2*A*, *middle panel*).

We then analyzed GR recruitment to the P4 region. Unexpectedly, ChIP assays performed 30 min after treatment with Dex demonstrated that there was no GR binding to the *bcl-X* P4 region (Fig. 2*B*, *upper panel*, compare *lanes 1* and *2*). No differences in the binding of GR were observed either in the *bcl-X* proximal promoter region encompassing P1 (Fig. 2*B*, *lower panel*). The *GAPDH* gene was used as control (Fig. 2*B*, *middle panel*).

The same result was also observed in the T lymphocyte derivative cell line S49, which is known to respond to glucocorticoids with programmed cell death (19, 20). In these cells we performed a time-course analysis of the sequence of events at P4 region following hormone treatment. The results show that GR is bound transiently to *bcl-X* P4 reaching a maximal binding between 10 and 15 min after Dex addition and leaving the promoter after 25 min (Fig. 2*C*, *upper panel*, *lanes 1–7*).

Binding of GR to P4 was accompanied by the recruitment of the co-activator SRC-1, the chromatin remodeling complex BRG-1 and pol II, which peaked 10–15 min after hormone treatment and thereafter returned to basal levels (Fig. 2*C*, *second*, *third*, and *fourth panels*, respectively). None of these changes were detected in the proximal promoter region containing P1 (Fig. 2*C*, *even panels*). Taken together, these results suggest a transient and selective activation followed by a stable repression of P4 after hormone treatment.

STAT5B Mediates the Hormonal Inhibition of P4 Activity—A sequence analysis of the P4 region revealed the presence of a putative STAT5 half site, 5′-TTCtgtGAA-3′ (Fig. 3*A*), which is well conserved when compared with a *consensus* STAT5B binding sequence (TTCnnnGAA) (33). This potential STAT5 site is located 213 bp upstream of the P4 TATA box, 63 bp downstream from HRE II, which we have recently identified (15), and overlaps HRE II described by Gascoyne *et al.* (7).

To test the effect of STAT5 on the hormone-dependent activity of P4, the expression vector pP4-extended (wt), containing the luciferase reporter gene under the control of P4, was co-transfected with a GR-expressing vector and increasing amounts of constitutively active pSTAT5A or pSTAT5B vectors in COS-1 cells. COS-1 cells were used because they do not express endogenous STAT5 factors. In these cells, Dex activates the transfected *bcl-X* reporter gene (4.0 ± 0.2).[4] Fig. 3*B* represents the effect of STAT5A or STAT5B on the expression of the reporter gene pP4-extended (wt) and shows a drastic and significant dose-dependent inhibition of the hormone-induced P4 activity by STAT5B (0.9 ± 0.2) and a weaker but also significant effect of STAT5A (2.4 ± 0.1, Fig. 3*B*, *lower* and *upper curves*, respectively). Overexpression of any of the two STAT5 isoforms in the absence of GR did not affect the basal P4 activity (data not shown). These results suggest that the putative STAT5 site on P4 region could mediate the hormonal repression of the promoter.

To test the functional relevance of the STAT5 site, we performed transient co-transfection assays in COS-1 cells with a GR vector, the mutated expression vector pP4ΔSTAT5 (mut),

[4] L. Rocha-Viegas, personal communication.

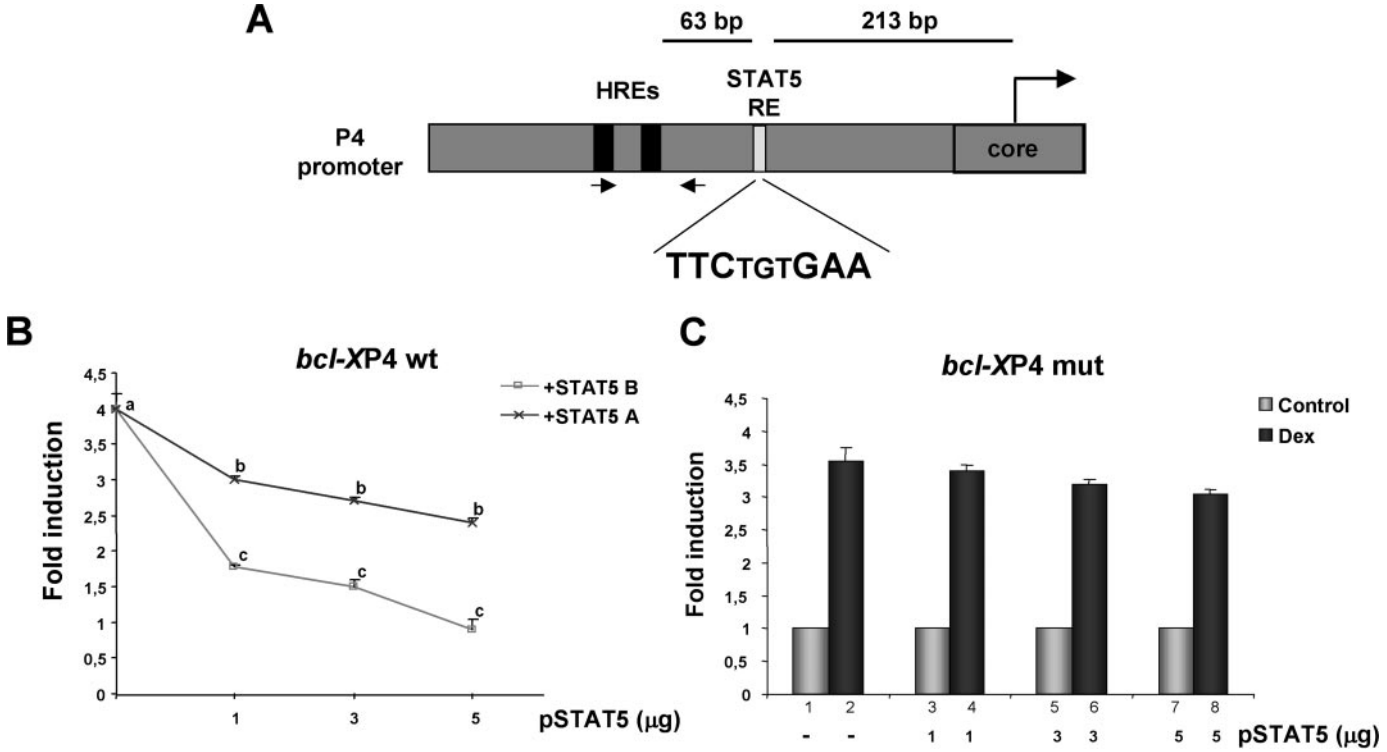

FIGURE 3. **Location, sequence, and function of the STAT5 response element in the 5′-flanking region of P4.** *A*, the diagram shows the extended P4 region with the location of both HREs and the STAT5-responsive element indicated. The *arrows* denote the location of the oligonucleotides used for ChIP experiments. *B* and *C*, COS-1 cells were co-transfected with 3 μg of pP4-extended reporter vector (*wt*) (*B*) or pP4ΔSTAT5 (*mut*) (*C*), 1 μg of pGR and increasing amounts of pSTAT5 vectors. Three micrograms of pCMV-LacZ was used as control of transfection. Cells were incubated for 36 h with and without Dex and luciferase activity was measured. β-Galactosidase activity was used to correct for transfection efficiency. The values are expressed as -fold induction relative to the controls. The means ± S.E. from three independent experiments are shown. *Bars* with *different superscript letters* are significantly different from each other ($p < 0.01$).

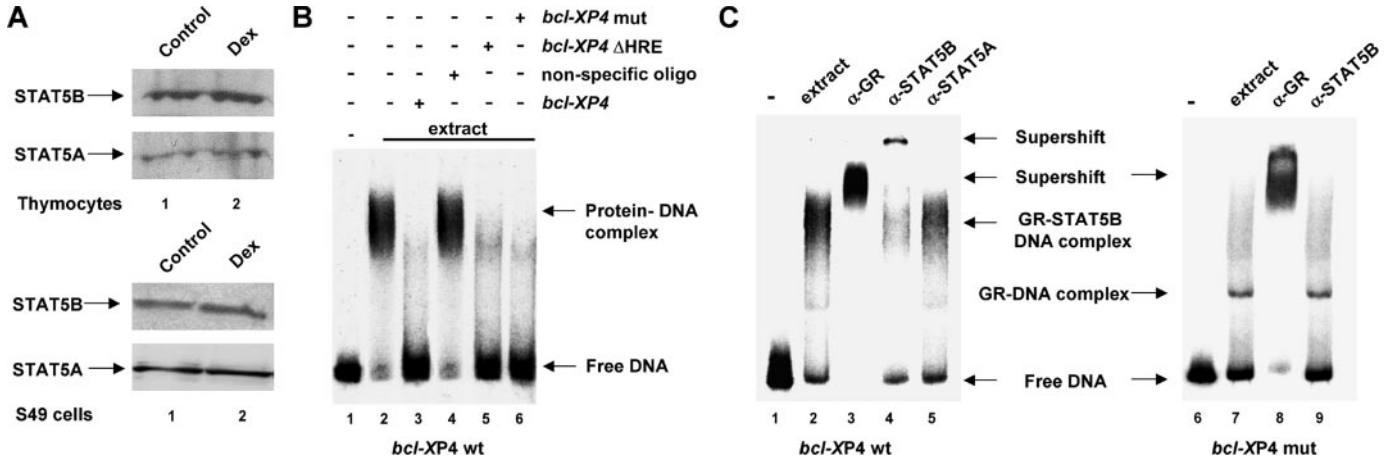

FIGURE 4. *A*, Western blot of STAT5A and STAT5B in thymocytes (*upper panels*) and S49 cells (*lower panels*) incubated without (*lane 1*) or with Dex (*lane 2*). *B* and *C*, EMSA performed with nuclear extracts from S49 cells incubated with Dex for 30 min and a ^{32}P-radiolabeled oligonucleotide containing the *bcl-XP4* wild type (*B*, *lanes 2–6* and *C*, *lanes 2–5*) or mutated (C, *lanes 7–9*). *B*, competition with a 500-fold molar excess of unlabeled *bcl-XP4* wt (*lane 3*), nonspecific oligonucleotide (*lane 4*), *bcl-XP4*ΔHRE (*lane 5*), and *bcl-XP4*mut (*lane 6*). *C*, supershift assays performed with α-GR (*lane 3* and *8*); α-STAT5A (*lane 5*) or α-STAT5B (*lane 4* and *9*). *Lanes 1* and *6* correspond to incubation without nuclear extract. The *arrows* indicate the free, shifted, and supershifted DNA. The results correspond to representative gels from three independent experiments.

which contains four point mutations on the P4 STAT5 putative site that should disrupt its DNA binding (33), and increasing amounts of the constitutively active pSTAT5B vector. Hormonal treatment increased this construct activity 3.50 ± 0.02-fold (Fig. 3*C*, *lane 2*); however, STAT5B did not affect hormone responsiveness to the same extent as seen with the wild-type P4 promoter (Fig. 3*C*, *lanes 4*, *6*, and *8*). These results suggest a role for the STAT5-DNA binding element in the negative regulation by STAT5B of glucocorticoid-induced P4 activity.

We next analyzed whether mouse thymocytes and S49 cells express STAT5 factors. Western blot analysis demonstrated that both STAT5 isoforms, A and B, are present in both cell types and their levels were not affected by Dex treatment (Fig. 4*A*, *upper* and *lower panels*, respectively). Therefore, STAT5 factors could participate in the hormone-

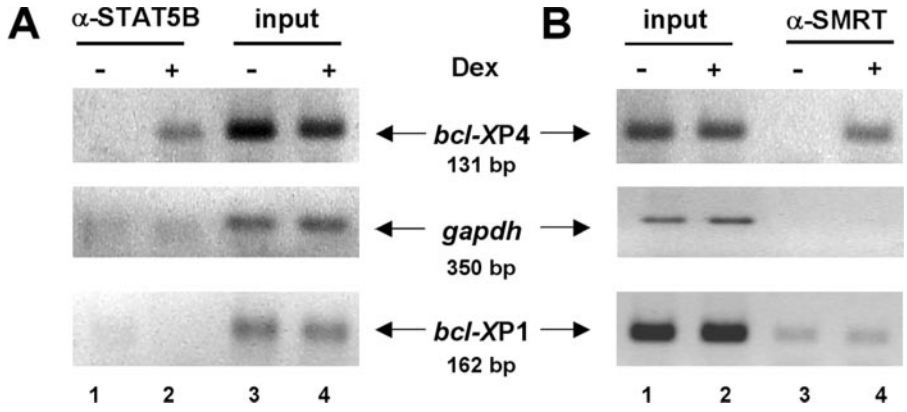

FIGURE 5. **Binding of STAT5B (*A*) and SMRT complex (*B*) to *bcl-X* P4 region (*upper panels*) and to *bcl-X* P1 region (*lower panels*) determined by ChIP assays of thymocytes from animals treated without or with Dex for 30 min.** *GAPDH* gene amplification was used as control (*middle panels*). The results correspond to representative gels from three independent experiments. *bp*, base pairs.

mediated inhibition of P4 via its interaction with the putative STAT5 binding site.

To test this possibility, we performed EMSAs with nuclear extracts from Dex-treated cells and a labeled fragment of *bcl-XP4* (wt), including the HREs and the STAT5 site. The nuclear extracts were obtained from S49 cells treated during 30 min with Dex. The EMSAs showed a strong and broad retarded complex (Fig. 4, *B* and *C*, *lane 2*). In binding competitions experiments, not only the unlabeled *bcl-XP4*wt, but also the *bcl-XP4*ΔHRE and *bcl-XP4*mut (carrying the four point mutations of the STAT5 binding site described above) were strong competitors of the labeled *bcl-XP4*wt fragment (Fig. 4*B*, *lanes 3*, *5*, and *6*, respectively), suggesting that both proteins should be present to form the complex. Moreover, it was effectively supershifted with a monoclonal GR antibody (Fig. 4*C*, *lane 3*) and less effectively with a monoclonal STAT5B antibody (Fig. 4*C*, *lane 4*) but not with a polyclonal antibody against STAT5A (Fig. 4*C*, *lane 5*). The EMSAs performed with nuclear extract from untreated cells did not show any complex formation (data not shown). These results suggest that both GR and STAT5B bind simultaneously to the same promoter fragment *in vitro*. Similar results were obtained with nuclear extracts from thymocytes derived from mice treated for 30 min with Dex (data not shown). To test the specificity of the binding we used the labeled *bcl-XP4*mut fragment. On this promoter, the S49 nuclear extract generated a faster migrating retarded band (Fig. 4*C*, *lane 7*), which was supershifted by a GR antibody (Fig. 4*C*, *lane 8*), but not with a STAT5B antibody (Fig. 4*C*, *lane 9*) and therefore corresponds to a GR containing complex. This complex was also observed in EMSAs performed with recombinant GR (15). These results demonstrate that both GR and STAT5B are present in nuclear extracts from hormone-treated cells and can bind simultaneously to naked P4 DNA. Moreover, the *in vitro* binding of STAT5B requires the integrity of the putative STAT5 binding site.

In Vivo Recruitment of STAT5B and SMRT to P4 upon Dex Treatment—We next investigated a direct participation of STAT5B in P4 regulation using ChIP assays. In thymocytes from control mice, very little, if any, STAT5B was found bound to P4 region (0.06% DNA bound, Fig. 5*A*, *upper panel*, *lane 1*). After 30 min of hormone treatment, STAT5B was found bound to P4 region (3.0% DNA bound, Fig. 5*A*, *upper panel*, *lane 2*). *GAPDH* was used as control (Fig. 5*A*, *middle panel*). Independently of hormone treatment, no STAT5B was bound to the *bcl-X* proximal promoter region encompassing P1 (Fig. 5*A*, *lower panel*). On the other hand, no recruitment of STAT5A to P4 region was detected in thymocytes from control or treated mice (data not shown). This result suggests that hormone-dependent selective recruitment of STAT5B to P4 region could be involved in the hormonal repression of *bcl-X* transcription.

To start defining the mechanism of repression, we analyzed the contribution of co-repressor complexes. In a previous report, the nuclear receptor co-repressor SMRT was identified as a potential STAT5-binding partner (34). We therefore tested whether SMRT was recruited to P4 upon hormonal treatment. ChIP experiments with a specific antibody showed that SMRT was recruited to P4 in thymocytes from mice treated with Dex for 30 min (2.1% DNA bound, Fig. 5*B*, *upper panel*, *lane 4 versus lane 3*). *GAPDH* was used as control (Fig. 5*B*, *middle panel*). No changes in the binding of SMRT complex to *bcl-X* proximal promoter region were observed (0.7% and 0.5% DNA bound for control and Dex-treated thymocytes, respectively, Fig. 5*B*, *lower panel*).

Similar results were obtained with the S49 cell line. In fact, the kinetics of binding of STAT5B in this cell type showed that STAT5B was also rapidly recruited to P4 (Fig. 6*A*, *first panel*, *lanes 1–7*), but, in contrast with GR, it remained bound for at least 30 min. Thus, between 5 and 25 min both factors were present simultaneously at P4 (compare the *first panels* of Figs. 6*A* and 2*C*). Although STAT5 proteins have been reported to form heterodimers with GR in different cell types (35–38), we were not able to co-precipitate phosphorylated STAT5B and GR upon hormone treatment (data not shown).

Thus, we next searched an explanation for the transient binding of GR. The SMRT co-repressor complex was recruited to the P4 region 25 min after hormone treatment, coinciding with the release of GR (Fig. 6*A*, *second panel*, *lane 6*, compare with the same lane in Fig. 2*C*, *upper panel*), suggesting a causal relationship between these two events. Thus, SMRT complex could participate in the STAT5B-mediated hormonal repression of P4 promoter in both thymocytes and S49 cells. No changes in the binding of STAT5B and SMRT complex to *bcl-X* proximal promoter region were observed following hormone treatment (Fig. 6*A*, *even panels*). STAT5A was not recruited to P4 region in this cell line (data not shown).

The SMRT complex is known to contain HDAC3, whose deacetylase activity is required for repression (39, 40). Indeed, 30 min after hormone treatment, the P4 region of S49 cells was enriched in HDAC3 (1.3 ± 0.1% and 3.3 ± 0.9% DNA bound for control and Dex-treated cells, respectively) (Fig. 6*B*, *upper panel*, *lane 2 versus lane 1*), and the levels of histone H3 acety-

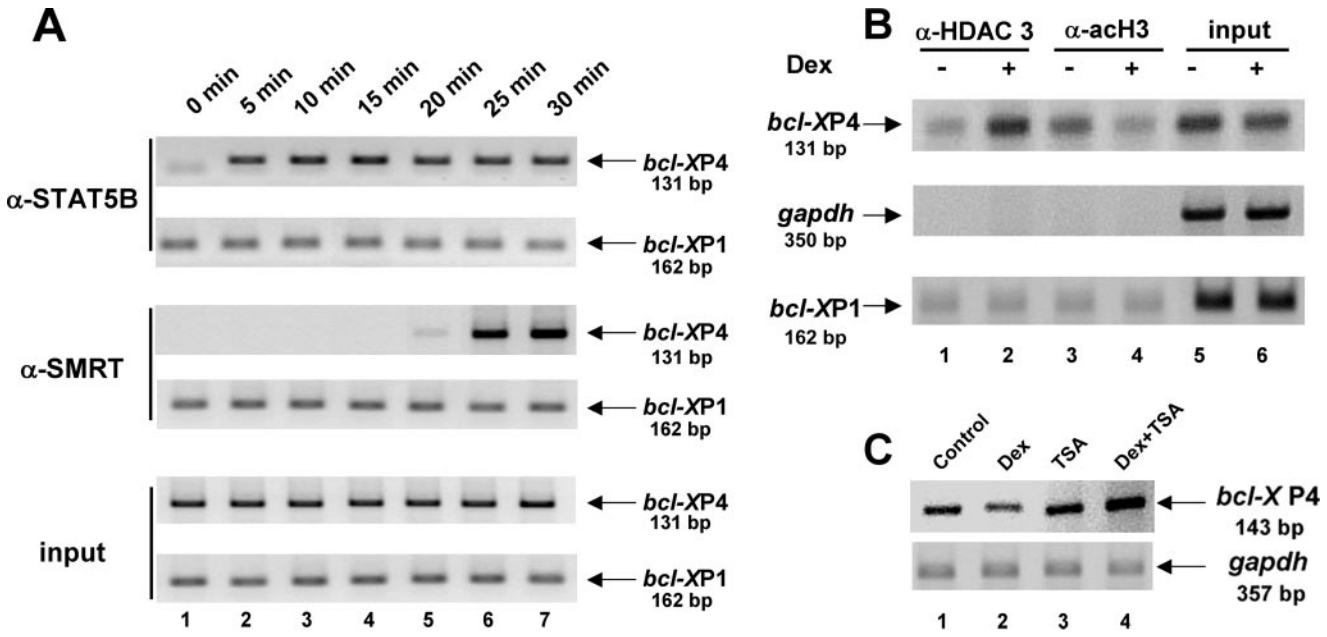

FIGURE 6. *A*, kinetics of STAT5B and SMRT binding to P4. S49 cells incubated from 5 to 30 min with Dex (*lanes 2–7*, *odd panels*) and P1 regions (*even panels*) determined by ChIP assays. Input chromatin is shown in the *last panels*. *B*, ChIPs assays performed with antibodies α-HDAC3 (*lanes 1* and *2*) and α-acetylated histone 3 (α-acH3, *lanes 3* and *4*) to P4 (*odd panels*) or P1 (*even panels*) in S49 cells incubated for 30 min with (*lanes 2*, *4*, and *6*) or without Dex (*lanes 1*, *3*, and *5*). *C*, amplification of *bcl-X* P4 leading exon (*upper panel*) by reverse transcription-PCR of total RNA from S49 cells, incubated for 5 h without (*lanes 1* and *3*) or with Dex (*lanes 2* and *4*) in the absence (*lanes 1* and *2*) or presence of 16 μM TSA (*lanes 3* and *4*). 10 μl of PCR products was electrophoresed in 1.6% agarose gel. *GAPDH* cDNA amplification was used as control (*lower panel*). The results correspond to representative gels from three independent experiments. *bp*, base pairs.

lation were decreased (2.5 ± 0.3% and 1.6 ± 0.1% DNA bound for control and Dex-treated cells, respectively, Fig. 6*B*, *upper panel*, *lane 4 versus lane 3*). No such changes were detected in *bcl-X* proximal promoter region (Fig. 6*B*, *lower panel*). This result suggests that compaction of chromatin may be the reason for the release of GR, SRC-1, BRG-1, and pol II, and therefore for repression of P4 activity.

To test this possibility we analyzed whether deacetylase activity is required for P4 repression. Therefore, we studied the influence of the HDAC inhibitor TSA, on Dex-mediated P4 transcriptional activity in S49 cells. The reverse transcription-PCR assays confirmed that Dex represses P4 activity (0.67 of control, Fig. 6*C*, *lane 2 versus lane 1*). This repression was reverted to activation in the presence of the HDAC inhibitor (1.45-fold induction, comparing Dex plus TSA *versus* TSA, Fig. 6*C*, *lane 4 versus lane 3*). TSA alone increased P4 activity 1.5-fold induction, comparing TSA *versus* Control (Fig. 6*C*, compare *lane 3 versus lane 1*). The *GAPDH* gene was used as control (Fig. 6*C*, *lower panel*). We conclude that histone deacetylation contributes to the transcriptional repression of *bcl-X* P4 in response to glucocorticoids.

Inhibition of STAT5 Activation Converts Glucocorticoids into Activators of P4 Promoter—It is known that STAT5 factors are phosphorylated by an activated JAK to reach the nucleus and be recruited by chromatin (36). On the other hand, it has been reported that STAT5 factors are activated in several cell types treated with glucocorticoids (35–38).

Therefore, we then analyzed by immunoprecipitation assays followed by Western blot the hormone effect on the phosphorylation level of STAT5B in S49 cells and thymocytes. The results showed that STAT5B is phosphorylated in both cell types independently of the hormonal treatment (Fig. 7*A*, *lane 1 versus lane 2*, and data not shown), thus the glucocorticoid-mediated repression of P4 might be dependent of the presence of an activated STAT5B factor. We then analyzed whether STAT5B phosphorylation is required for P4 repression. Therefore, we studied the influence of the JAK inhibitor AG490 on Dex-induced recruitment of STAT5B to P4 in S49 cells. As control, the phosphorylation state of STAT5B was tested (Fig. 7*A*, compare *lane 5 versus lane 4*). STAT5B did not bind to P4 region when cells were incubated with AG490 alone (Fig. 7*B*, *upper panel*, *lane 3*). Pre-treatment with the inhibitor abolished the recruitment of STAT5B to P4 region that was observed in cells treated during 30 min with Dex alone (Fig. 7*B*, *upper panel*, compare *lanes 2* and *4*). Similarly, binding of SMRT to P4 promoter did not change in S49 cells treated for 30 min with Dex in the presence of the JAK inhibitor (0.07% DNA bound for hormone-untreated and hormone-treated cells) (Fig. 7*B*, *upper panel*, *lanes 1* and *2*, respectively), whereas it was increased in the absence of the inhibitor (0.72% DNA bound for hormone-untreated cells and 3.03% DNA bound for hormone-treated cells, respectively, Fig. 7*B*, *upper panel*, *lanes 3* and *4*).

In the presence of the JAK inhibitor we found that GR was recruited to P4 30 min after hormone addition (3.61% DNA bound *versus* 0.01% DNA bound for cells treated with AG 490 alone, Fig. 8*A*, *upper panel*, *lanes 4* and *3*, respectively). By contrast, in controls not treated with AG490, GR was not found at P4 promoter after 30 min of Dex treatment (see Fig. 2*C*, *first panel*, *lanes 1* and *7*). Moreover, under these conditions control S49 cells did not recruit GR to P4 region compared with the *in vivo* data (compare with Fig. 2*B*). Taken together, these findings support the notion that recruitment of

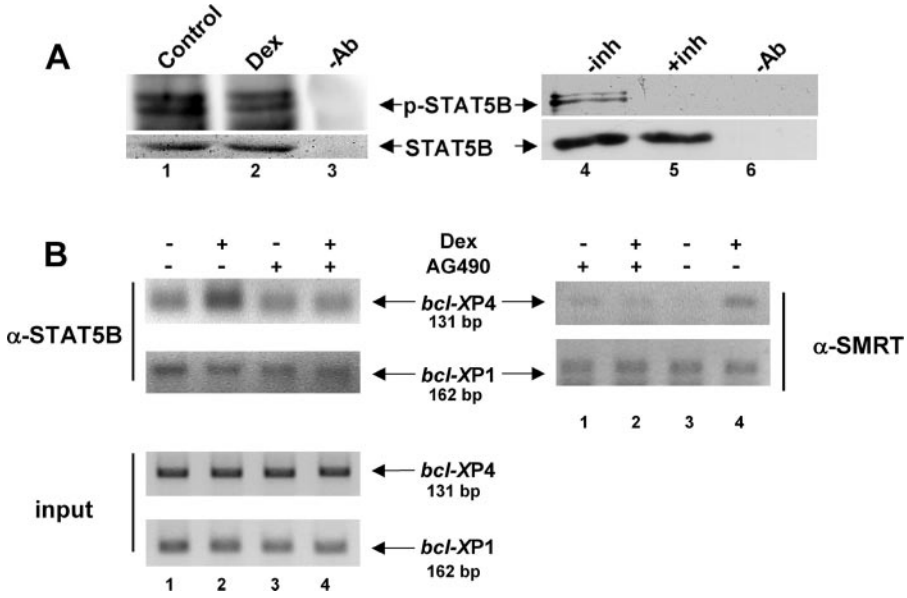

FIGURE 7. *A*, immunoprecipitation assays with antibodies α-STAT5B (*lanes 1*, *2*, *4*, and *5*) or no immune serum (*lane 3* and *6*) of S49 cells incubated for 15 min without (*lane 1*) or with Dex (*lanes 2–6*) in the absence (*lanes 1–4*) or presence of 100 μM AG490 JAK inhibitor (added 2 h before Dex) (*lanes 5* and *6*). The immunoprecipitates were analyzed by Western blot with α-P-tyrosine. α-STAT5B was used as control. *B*, binding of STAT5B (*left panels*) and SMRT (*right panels*) to *bcl-X* P4 (*upper panels*) and to P1 region (*lower panels*) determined by ChIP assays in S49 cells incubated for 30 min without (*lanes 1* and *3*) or with Dex (*lanes 2* and *4*) in the presence or absence of 100 μM AG490 (added 2 h min before Dex). *Left lower panels*: input chromatin. The results correspond to representative gels from three independent experiments. *bp*, base pairs. *inh*, inhibitor.

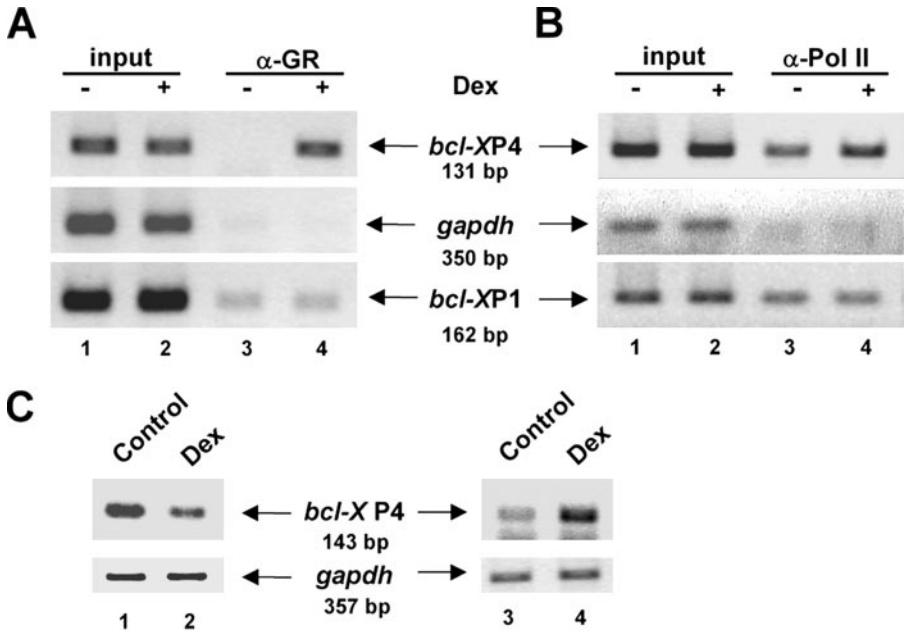

FIGURE 8. **Effect of inhibiting JAK activity on bcl-X P4 activation.** *A* and *B*, S49 cells were incubated for 30 min without (*lanes 1* and *3*) or with Dex (*lanes 2* and *4*) in the presence of 100 μM AG490. Binding of GR (*A*) and pol II (*B*) to *bcl-X* P4 (*upper panels*) and to P1 region (*lower panels*) determined by ChIP assays. *Lanes 1* and *2*, input chromatin. *GAPDH* gene amplification was used as control (*middle panels*). *C*, amplification of *bcl-X* P4 leading exon (*upper panels*) by reverse transcription-PCR of total RNA from S49 cells, incubated for 5 h without (*lanes 1* and *3*) or with Dex (*lanes 2* and *4*) in the absence (*lanes 1* and *2*) or presence of 100 μM AG490 (*lanes 3* and *4*). 10 μl of PCR products was electrophoresed in 1.6% agarose gel. *GAPDH* cDNA amplification was used as control (*lower panels*). The results correspond to representative gels from three independent experiments. *bp*, base pairs.

phosphorylated STAT5B and SMRT complex suppresses binding of GR to P4 promoter.

We next tested whether the *bcl-X* P4 region was transcriptionally active in the presence of the JAK inhibitor. ChIP experiments using a monoclonal pol II antibody showed that the inhibition of pol II binding to P4 provoked by the hormone treatment was abolished when the cells were co-incubated with the JAK inhibitor (Fig. 8*B*, *upper panel*, *lanes 3* and *4*, respectively, compare with Fig. 2*C*, *fourth panel*, *lanes 1* and *7*). Instead, a small increase in pol II recruitment was observed (1.63% for hormone-untreated cells and 2.46% for hormone-treated cells, respectively), which was not found in the proximal promoter region (Fig. 8*B*, *lower panel*). The incubation with AG490 did not change pol II binding to *GAPDH* control promoter (Fig. 8*B*, *middle panel*). Transcriptional activation of P4 promoter under these conditions was confirmed by reverse transcription-PCR. Thus, the repressive effect of Dex on P4 activity (Fig. 8*C*, *lane 2 versus lane 1*) was reverted to activation (2.8-fold induction, Fig. 8*C*, *lane 4 versus lane 3*) in the presence of the JAK inhibitor.

DISCUSSION

It is well known that glucocorticoids induce apoptosis in most nucleated cells of vascular system (1). However, there is evidence for an opposite action in other cell types, such as glandular cells, where glucocorticoids protect against programmed cell death (2, 5–7). An intriguing question arises concerning the mechanism by which the cell phenotype determines the final effect of glucocorticoids on apoptosis (1). Considerable effort has been devoted to the identification of target genes involved on glucocorticoid-mediated cell death (1, 8, 17). It is known that glucocorticoids promote apoptosis through induction of proapoptotic Bcl-2 family proteins, such as Bad in thymocytes (41), or through reduction in the expression of survival members, like Bcl-2 and Bcl-X_L in leukemic cells (42, 43). Our group demonstrated that both *bcl-X* expression and the relative level of the antiapoptotic isoform *bcl-*X_L are under hormonal control in a cell type-dependent manner (4, 15, 16). Whereas in endometrial cells glucocorticoids activate

bcl-X expression, lead to a relative accumulation of *bcl-X_L*, and inhibit apoptosis (4), in thymocytes glucocorticoids repress *bcl-X* expression, diminish the relative level of *bcl-X_L*, and induce apoptosis (Refs. 16 and 17 and this report). Thus, *bcl-X* is at least one target gene whose differential control in different cell types is involved in both the antiapoptotic and the apoptotic effects of steroid hormones.

Recently, we have demonstrated that the region located immediately upstream of P4 promoter contains two hormone response elements, which bind glucocorticoid receptor and confer *in vivo* hormone responsiveness to the core promoter (15). As a consequence, this promoter is directly activated upon hormonal treatment of mammary epithelial cells, and this effect correlates with an increased *bcl-X_L* mRNA.

Conversely, we show here that glucocorticoids decrease both *bcl-X_L* mRNA and Bcl-X_L protein levels and repress P4 activity on mouse thymocytes. Thus, the changes in the transcription factor occupancy of the P4 promoter would influence the overall expression of Bcl-X protein and the regulation of apoptosis. We should note that, in addition to the transcriptional regulation, Bcl-X function also is regulated by proteolytic cleavage and subcellular localization (44); however, because the Bcl-X_L protein levels decrease was detected only after 8 h of hormone addition, it seems unlikely that Dex would directly affect Bcl-X protein stability.

bcl-X_L repression correlates with the recruitment of STAT5B protein to a novel STAT5 binding site located 213 bp upstream of P4 TATA box. This new STAT5 site confers glucocorticoid-dependent repression to P4 and points to a more complex hormonal regulation of *bcl-X* transcription than that previously shown in growing cultured mammary epithelial HC11 cells, which do not express STAT5B (2, 15).

Although it has been demonstrated that both STAT5 isoforms are more than 90% identical (45), STAT5A and STAT5B are not functionally identically. Differences in the functionality between both isoforms were reported in adipocytes (46) and in the mammary gland (36). Here we demonstrate that, although both STAT5 proteins are expressed on mouse thymocytes and S49 T cells, only STAT5B is recruited to P4 region upon Dex addition.

Several groups have reported interactions between GR and STAT5 factors in different cell types (35–38). In particular, an interplay between lymphokines and glucocorticoids in the control of thymocyte apoptosis has been described. Cytokines interfere with glucocorticoid signaling in the immune system by activation of the JAK/STAT signaling pathway (47). It was suggested that the STAT5-repressive activity on glucocorticoid-dependent transcription in this tissue is dependent on the promoter context and STAT5 activation level and may involve direct interaction of STAT5 with GR (47).

The question arises as to whether GR and STAT5B reach *bcl-X* P4 region as a heterodimer or whether both transcription factors are individually targeted to the promoter upon hormone treatment. It is known that STAT5 factors are activated in several cell types treated with glucocorticoids and that they can form heterodimers with GR (35–38). However, because our results show that STAT5B is phosphorylated independently of the presence of Dex and it does not seem to interact with the ligand-activated GR, it is possible that both factors bind to the P4 region independently, although we cannot exclude that the fraction of STAT5B interacting with GR is too small to be detected in co-immunoprecipitation experiments.

Whether a heterodimer is formed or not, targeting could be either via the HREs and/or via the STAT5 binding element. The ChIP experiments do not directly address the function of these sites, a question that cannot be addressed in transient transfection experiments, because chromatin is not properly organized on transfected DNA. However, both GR and STAT5B bind simultaneously to the same promoter fragment *in vitro*, and the HREs and the STAT5 binding site are necessary for generation of the retarded protein-DNA complexes. On the other hand, not only EMSAs performed with the labeled *bcl-XP4* mutated fragment but also experiments with the inhibitor of STAT5 activation suggest that ligand-activated GR has the potential to target *bcl-XP4* independent of STAT5B, although we do not know whether this potential is used in the absence of the inhibitor. The differences in the GR and STAT5B binding observed between EMSA and ChIPs assays suggest that chromatin structure plays a role in P4 regulation.

Transcriptional repression of *bcl-X* P4 by Dex in thymocytes follows a rapid recruitment of GR and a combination of factors involved in transcriptional activation, including SRC-1, a transcriptional co-activator; BRG-1, a component of an ATP-dependent chromatin remodeling complex; and pol II. These indicators of gene activation are bound to P4 region for only a short time, which likely is insufficient to result in a significant accumulation of the corresponding transcripts. The role of the transient recruitment of GR is not clear yet. One possibility is that GR helps recruitment of STAT5B to the P4 region. Because the hormonal treatment neither induces STAT5B/GR interactions nor affects STAT5B phosphorylation state, the effect of GR may be indirect. For instance, transient recruitment of BRG-1 by GR could be sufficient to promote a wave of chromatin remodeling that would allow STAT5B to gain access to its target sequences. This is reminiscent of the situation on the murine mammary tumor virus promoter, where NF1 recruitment depends on a previous binding of hormone receptors to accessible HREs followed by receptor-dependent chromatin remodeling (48). In that sense, a transient activation could be necessary for further repression initiated by STAT5B. Concerning the mechanism of repression, our results show that STAT5B is stably recruited to P4 region along with GR. 20 min after STAT5B binding, SMRT co-repressor and HDAC3 are recruited to the promoter and concomitantly histone H3 is partially deacetylated. Thus SMRT could be responsible for transcriptional repression of P4 activity. SMRT is known to interact with STAT5 (34), and overexpression of SMRT suppresses interleukin-3 induction of STAT5 target genes (34).

The mechanism leading to GR displacement from the P4 region is not clear. It is possible that GR binds naturally in waves, the first lasting for only 15–20 min, in a way similar to that reported for binding of the estrogen receptor to the pS2 promoter (49). Moreover, on the murine mammary tumor

virus promoter, it was proposed that GR is actively assisted by nucleosome remodeling both in the binding and displacement from a target promoter (50). These authors also suggest that receptor-directed actions probable result from many repeated short-lived GR-DNA interactions rather than from the formation of stable multiprotein complexes during chromatin remodeling (50). If the first wave of GR binding would enable access of STAT5B and recruitment of SMRT, an active competition between GR and SMRT for binding STAT5B, or the resulting compaction of chromatin could prevent further waves of GR binding. Chromatin compaction is a plausible model, supported by the demonstration that the HDAC inhibitor, TSA, reverted Dex-mediated repression to activation. We cannot discard the notion that other mechanisms may be involved in P4 repression as in the transient transfection assays we also observed a decrease in luciferase activity. However, it should be noted that unphysiological amounts of transcription factors are added in these assays, and the results might not be comparable with *in vivo* analysis of endogenous gene expression. On the other hand, the glucocorticoid-dependent repression of *bcl-X*$_L$ could be mediated by induction of the GILZ transcription factor (17). GILZ was first isolated as a Dex-responsive gene from a thymus subtraction library (51), and it was reported to interfere at various stages of the glucocorticoid signal transduction pathway by interacting with other transcription factors (52, 53). Because GILZ can bind to a gene promoter as a transcriptional repressor (54), our results provide a basis for studying the role of GILZ in P4 repression. The final consequence of these changes in P4 promoter is a decrease in the accumulation of the transcripts derived from it with the corresponding decrease in the proportion of the *bcl-X*$_L$ isoform.

Acknowledgments—We thank Dr. T. Kitamura, Institute of Medical Science, University of Tokyo, Japan for the STAT5 vectors, Dr. J. M. Hardwick, The Johns Hopkins Hospital, Baltimore, MD for pGLD3 vector, and Med. Vet. María Croce for technical assistance.

REFERENCES

1. Amsterdam, A., Tajima, K., and Sasson, R. (2002) *Biochem. Pharmacol.* **64,** 843–850
2. Schorr, K., and Furth, P. A. (2000) *Cancer Res.* **60,** 5950–5953
3. Berg, M. N., Dharmarajan, A. M., and Waddell, B. J. (2002) *Endocrinology* **143,** 222–227
4. Pecci, A., Scholz, A., Pelster, D., and Beato, M. (1997) *J. Biol. Chem.* **272,** 11791–11798
5. Hillier, S. G., and Tetsuka, M. (1998) *J. Reprod. Immunol.* **39,** 21–27
6. Yamamoto, M., Fukuda, K., Miura, N., Suzuki, R., Kido, T., and Komatsu, Y. (1998) *Hepatology* **27,** 959–966
7. Gascoyne, D. M., Kypta, R. M., and Vivanco, M. M. (2003) *J. Biol. Chem.* **278,** 18022–18029
8. Lotem, J., and Sachs, L. (1995) *Cell Growth & Differ.* **6,** 647–653
9. Hoijman, E., Rocha Viegas, L., Keller Sarmiento, M. I., Rosenstein, R. E., and Pecci, A. (2004) *Endocrinology* **145,** 418–425
10. Boise, L. H., Gonzalez-Garcia, M., Postema, C. E., Ding, L., Lindsten, T., Turka, L. A., Mao, X., Nunez, G., and Thompson, C. B. (1993) *Cell* **74,** 597–608
11. Fang, W., Rivard, J. J., Mueller, D. L., and Behrens, T. W. (1994) *J. Immunol.* **153,** 4388–4398
12. Shiraiwa, N., Inohara, N., Okada, S., Yuzaki, M., Shoji, S., and Ohta, S. (1996) *J. Biol. Chem.* **271,** 13258–13265
13. Yang, X. F., Weber, G. F., and Cantor, H. (1997) *Immunity* **7,** 629–639
14. Schmitt, E., Paquet, C., Beauchemin, M., and Bertrand, R. (2004) *Oncogene* **23,** 3915–3931
15. Viegas, L. R., Vicent, G. P., Baranao, J. L., Beato, M., and Pecci, A. (2004) *J. Biol. Chem.* **279,** 9831–9839
16. Vicent, G. P., Pecci, A., Ghini, A., Piwien-Pilipuk, G., and Galigniana, M. D. (2002) *Exp. Cell Res.* **276,** 142–154
17. Delfino, D. V., Agostini, M., Spinicelli, S., Vito, P., and Riccardi, C. (2004) *Blood* **104,** 4134–4141
18. Pecci, A., Viegas, L. R., Baranao, J. L., and Beato, M. (2001) *J. Biol. Chem.* **276,** 21062–21069
19. Hyman, R. (1973) *J. Natl. Cancer Inst.* **50,** 415–422
20. Gehring, U., Ulrich, J., and Segnitz, B. (1982) *Mol. Cell Endocrinol.* **28,** 605–611
21. Heermeier, K., Benedict, M., Li, M., Furth, P., Nunez, G., and Hennighausen, L. (1996) *Mech. Dev.* **56,** 197–207
22. Bottenstein, J., Hayashi, I., Hutchings, S., Masui, H., Mather, J., McClure, D. B., Ohasa, S., Rizzino, A., Sato, G., Serrero, G., Wolfe, R., and Wu, R. (1979) *Methods Enzymol.* **58,** 94–109
23. CCAC (1980) *Guide to the Care* and *Use of Experimental Animals*, Canadian Council of Animal Care, Ottawa
24. Godowski, P. J., Rusconi, S., Miesfeld, R., and Yamamoto, K. R. (1987) *Nature* **325,** 365–368
25. Ariyoshi, K., Nosaka, T., Yamada, K., Onishi, M., Oka, Y., Miyajima, A., and Kitamura, T. (2000) *J. Biol. Chem.* **275,** 24407–24413
26. Truss, M., Bartsch, J., Schelbert, A., Hache, R. J., and Beato, M. (1995) *EMBO J.* **14,** 1737–1751
27. Chomczynski, P., and Sacchi, N. (1987) *Anal. Biochem.* **162,** 156–159
28. Zinn, K., DiMaio, D., and Maniatis, T. (1983) *Cell* **34,** 865–879
29. Strutt, H., and Paro, R. (1999) *Methods Mol. Biol.* **119,** 455–467
30. Eberhardy, S. R., D'Cunha, C. A., and Farnham, P. J. (2000) *J. Biol. Chem.* **275,** 33798–33805
31. Quandt, K., Frech, K., Karas, H., Wingender, E., and Werner, T. (1995) *Nucleic Acids Res.* **23,** 4878–4884
32. Andrews, N. C., and Faller, D. V. (1991) *Nucleic Acids Res.* **19,** 2499
33. Ihle, J. N. (1996) *Cell* **84,** 331–334
34. Nakajima, H., Brindle, P. K., Handa, M., and Ihle, J. N. (2001) *EMBO J.* **20,** 6836–6844
35. Stocklin, E., Wissler, M., Gouilleux, F., and Groner, B. (1996) *Nature* **383,** 726–728
36. Cella, N., Groner, B., and Hynes, N. E. (1998) *Mol. Cell Biol.* **18,** 1783–1792
37. Debierre-Grockiego, F., Fuentes, V., Prin, L., Gouilleux, F., and Gouilleux-Gruart, V. (2003) *Br. J. Haematol.* **123,** 933–941
38. Tronche, F., Opherk, C., Moriggl, R., Kellendonk, C., Reimann, A., Schwake, L., Reichardt, H. M., Stangl, K., Gau, D., Hoeflich, A., Beug, H., Schmid, W., and Schutz, G. (2004) *Genes Dev.* **18,** 492–497
39. Guenther, M. G., Lane, W. S., Fischle, W., Verdin, E., Lazar, M. A., and Shiekhattar, R. (2000) *Genes Dev.* **14,** 1048–1057
40. Li, J., Wang, J., Nawaz, Z., Liu, J. M., Qin, J., and Wong, J. (2000) *EMBO J.* **19,** 4342–4350
41. Mok, C. L., Gil-Gomez, G., Williams, O., Coles, M., Taga, S., Tolaini, M., Norton, T., Kioussis, D., and Brady, H. J. (1999) *J. Exp. Med.* **189,** 575–586
42. Broome, H. E., Yu, A. L., Diccianni, M., Camitta, B. M., Monia, B. P., and Dean, N. M. (2002) *Leukocyte Res.* **26,** 311–316
43. Caron-Leslie, L. A., Evans, R. B., and Cidlowski, J. A. (1994) *FASEB J.* **8,** 639–645
44. Xue, L. Y., Chiu, S. M., Fiebig, A., Andrews, D. W., and Oleinick, N. L. (2003) *Oncogene* **22,** 9197–9204
45. Liu, X., Robinson, G. W., Gouilleux, F., Groner, B., and Hennighausen, L. (1995) *Proc. Natl. Acad. Sci. U. S. A.* **92,** 8831–8835
46. Floyd, Z. E., and Stephens, J. M. (2003) *Diabetes* **52,** 308–314
47. Biola, A., Lefebvre, P., Perrin-Wolff, M., Sturm, M., Bertoglio, J., and Pallardy, M. (2001) *Mol. Endocrinol.* **15,** 1062–1076
48. Di Croce, L., Koop, R., Venditti, P., Westphal, H. M., Nightingale, K. P., Corona, D. F., Becker, P. B., and Beato, M. (1999) *Mol. Cell* **4,** 45–54

49. Metivier, R., Penot, G., Hubner, M. R., Reid, G., Brand, H., Kos, M., and Gannon, F. (2003) *Cell* **115,** 751–763
50. Nagaich, A. K., Walker, D. A., Wolford, R., and Hager, G. L. (2004) *Mol. Cell* **14,** 163–174
51. D'Adamio, F., Zollo, O., Moraca, R., Ayroldi, E., Bruscoli, S., Bartoli, A., Cannarile, L., Migliorati, G., and Riccardi, C. (1997) *Immunity* **7,** 803– 812
52. Mittelstadt, P. R., and Ashwell, J. D. (2001) *J. Biol. Chem.* **276,** 29603–29610
53. Ayroldi, E., Migliorati, G., Bruscoli, S., Marchetti, C., Zollo, O., Cannarile, L., D'Adamio, F., and Riccardi, C. (2001) *Blood* **98,** 743–753
54. Shi, X., Shi, W., Li, Q., Song, B., Wan, M., Bai, S., and Cao, X. (2003) *EMBO Rep.* **4,** 374 –380

Genes: Structure and Regulation:

Glucocorticoids Repress *bcl-X* Expression in Lymphoid Cells by Recruiting STAT5B to the P4 Promoter

Luciana Rocha-Viegas, Guillermo P. Vicent, José L. Barañao, Miguel Beato and Adali Pecci

J. Biol. Chem. 2006, 281:33959-33970.
doi: 10.1074/jbc.M602408200 originally published online September 7, 2006